

OPEN ACCESS

Endothelial nitric oxide synthase is regulated by ERK phosphorylation at Ser⁶⁰²

John C. SALERNO*¹, Dipak K. GHOSH*, Raj RAZDAN*, Katy A. HELMS†, Christopher C. BROWN†, Jonathan L. McMURRY*, Emily A. RYE† and Carol A. CHRESTENSEN†

*Department of Biology, Kennesaw State University, Kennesaw, GA 30144, U.S.A.

†Department of Chemistry and Biochemistry, Kennesaw State University, Kennesaw, GA 30144, U.S.A.

Synopsis

eNOS (endothelial nitric oxide synthase) contains a MAPK (mitogen-activated protein kinase)-binding site associated with a major eNOS control element. Purified ERK (extracellular-signal-regulated kinase) phosphorylates eNOS with a stoichiometry of 2–3 phosphates per eNOS monomer. Phosphorylation decreases NO synthesis and cytochrome *c* reductase activity. Three sites of phosphorylation were detected by MS. All sites matched the SP and TP MAPK (mitogen-activated protein kinase) phosphorylation motif. Ser⁶⁰² lies at the N-terminal edge of the 42-residue eNOS AI (autoinhibitory) element. The pentabasic MAPK-binding site lies at the opposite end of the AI, and other critical regulatory features are between them. Thr⁴⁶ and Ser⁵⁸ are located in a flexible region associated with the N terminus of the oxygenase domain. In contrast with PKC (protein kinase C), phosphorylation by ERK did not significantly interfere with CaM (calmodulin) binding as analysed by optical biosensing. Instead, ERK phosphorylation favours a state in which FMN and FAD are in close association and prevents conformational changes that expose reduced FMN to acceptors. The close associations between control sites in a few regions of the molecule suggest that control of signal generation is modulated by multiple inputs interacting directly on the surface of eNOS via overlapping binding domains and tightly grouped targets.

Key words: eNOS, ERK, fluorescence lifetime, MAPK, nitric oxide synthase, phosphorylation

Cite this article as: Salerno, J.C., Ghosh, D.K., Razdan, R., Helms, K.A., Brown, C.C., McMurry, J.L., Rye, E.A. and Chrestensen, C.A. (2014) Endothelial nitric oxide synthase is regulated by ERK phosphorylation at Ser⁶⁰². *Biosci. Rep.* **34**(5), art:e00137.doi:10.1042/BSR20140015

INTRODUCTION

Signalling networks include elaborate feedback and feed-forward mechanisms and are responsible for homeostasis over multiple levels of organization. The familiar picture of signal transduction cascades in which amplification is obtained by sequential phosphorylation/activation has been augmented by the discovery of multi-component signalling complexes that may include receptors, kinases, scaffolds and adaptors, and non-kinase signal generators [1–4].

eNOS (endothelial nitric oxide synthase) is a signal generator in the regulation of vascular and airway tone, insulin secretion, angiogenesis and cardiac function [5–10]. Primary control is through Ca/CaM (calmodulin) activation [11], but numerous

other inputs have been described including inhibitory and activating phosphorylation by specific kinases, protein-protein interactions and cell trafficking. [12–15] Examples of activating kinases include PKA (protein kinase A), which phosphorylates Ser¹¹⁷⁹ and Ser⁶³⁵, and Akt, which phosphorylates Ser¹¹⁷⁹ and Ser⁶¹⁷ [15–18] (The sequence numbering of human and bovine eNOSs in the reductase regions differ by 2 amino acids; bovine Thr⁴⁹⁷ corresponds to human Thr⁴⁹⁵, bovine Ser⁶¹⁷ and Ser⁶³⁵ to human Ser⁶¹⁵ and Ser⁶³³ and bovine Ser¹¹⁷⁹ to human Ser¹¹⁷⁷; see also Figure 1). Ser¹¹⁷⁷ is located in the C-terminal tail, which acts to restrict the rate of haem reduction by the flavin containing domains [19–22]. Ser⁶³⁵ and Ser⁶¹⁷ are located in a large AI (autoinhibitory) insertion in the FMN-binding domain, which is displaced by CaM binding during activation [23]. PKC (protein kinase C) inhibits eNOS by phosphorylating Thr⁴⁹⁵ [24,25], adjacent to

Abbreviations: AI, autoinhibitory; Akt, PKB (protein kinase B); BAEC, bovine aortic endothelial cell; BH₄, tetrahydrobiopterin; BLI, biolayer interferometry; CaM, calmodulin; eNOS, endothelial nitric oxide synthase; ERK, extracellular-signal-regulated kinase; iNOS, inducible nitric oxide synthase; MAPK, mitogen-activated protein kinase; nNOS, neuronal nitric oxide synthase; NOS, nitric oxide synthase; PKA, protein kinase A; PKC, protein kinase C; SPR, surface plasmon resonance.

¹ To whom correspondence should be addressed (email: jsalern3@kennesaw.edu).

the CaM-binding site, which interferes with CaM-mediated activation [26,27]. Other phosphorylation sites associated with the oxygenase domain are less well studied.

MAPKs (mitogen-activated protein kinases), including ERK (extracellular-signal-regulated kinase), p38 and JNK (c-Jun N-terminal kinase) are important signalling nodes in pathways that control metabolism, growth and expression [28–32]. ERK and p38 both function in signalling pathways [33,34] that involve eNOS and good evidence for direct phosphorylation of eNOS by ERK1/2 in BAECs (bovine aortic endothelial cells) has been obtained [35]. Contradictory reports of the site of ERK phosphorylation have appeared [36,37]. The uncertainty is the result of pathway-dependent phosphorylation events in which ERK drives the activation of other kinases, since some of the proposed sites do not match the target motifs of MAPKs, and may also reflect cross-talk in which phosphorylation at one position exposes other positions to phosphorylation.

We recently identified a pentabasic-binding site for MAPKs in the eNOS AI element [38]. Here we report the sites of ERK phosphorylation, the effects on activity, and the mechanism by which phosphorylation regulates NO synthesis. The phosphorylation sites are distinct from the D-domain-type binding site we reported previously. The uncertainties introduced by pathway-dependent phosphorylation events have been removed by working with purified components, but additional sites might be exposed by covalent modification or protein–protein interactions in cells.

EXPERIMENTAL

Expression and purification of eNOS was carried out as previously described [37,39,40]. Prosthetic group content was measured spectrophotometrically [40]. NO synthase activity was measured using haemoglobin capture and Griess assay, and reductase activity was measured using cytochrome *c* reduction [41,42]. Affinity purified, single-band ERK2 from an *Escherichia coli* expression system was purchased from SignalChem.

ERK kinase reactions were performed in 20 mM Hepes (pH 7.4), 1 mM DTT, 10 mM MgCl₂, 1 mM ATP, 10% (v/v) glycerol and when using the high concentration eNOS, 0.75 mM EGTA. eNOS was used at various concentrations (45–1.6 μM for fluorescence and eNOS/cytochrome *c* experiments, respectively). Reactions were done plus or minus ERK (0.12–0.01 μM, depending on eNOS concentration) at room temperature, ~22 °C (see figure legends) and were ‘stopped’ by putting on ice until the activity was tested; within 5 h. 0.315 nM of phosphorylated and unphosphorylated eNOS were sent for MS analysis. MS of trypsin digested enzyme was carried out at the Emory University proteomics facility with duplicate phosphorylated and unphosphorylated samples.

Western blot analysis was done with a Li-Cor Odyssey. The control eNOS antibody was from Invitrogen (clone 9D10). The eNOS pS602 antibody is a peptide antibody. The phospho-

peptide, used to immunize rabbits, and the resulting antibodies were affinity purified by NeoBioLab.

BAECs were purchased from Lonza, grown in the recommended media and harvested at confluence using lysis buffer (50 mM Tris, 150 mM NaCl, 1.5 mM MgCl₂, 1% ipegal, 0.5% (v/v) Triton X-100, 2 mM EDTA, HALT protease inhibitor cocktail (Thermo) and 1 μM microcystin LR and 200 μM Na₃VO₄). Approximately 25% of the lysate from a 10 cm plate was treated with or without 400 units of λ phosphatase in a 50 μl reaction for the indicated times, 20 μl was loaded on the gel.

Time-resolved intensity decays were recorded using a PTI TC-SPC (time-correlated single-photon counting) fluorescence lifetime spectrometer as described [43]. FMN was excited at 473 nm using a pulsed laser diode with 20 MHz repetition rate; experiments with 378 nm excitation produced similar results. The decay of fluorescence can be represented as the sum of individual exponential decays:

$$I(t) = \sum_{i=1}^n \alpha_i \exp\left(-\frac{t}{\tau_i}\right) \quad (1)$$

where the τ_i are the decay times and α_i are the amplitudes of the *i*th component. The fractional contribution of the *i*th component in the steady state is:

$$f_i = \frac{\alpha_i \tau_i}{\sum_j \alpha_j \tau_j} \quad (2)$$

Individual values of α_i and τ_i were determined from simulation with PTI's Felix GX software with PowerFit 10 simulation module, using deconvolution of an instrument response function obtained from scattering and nonlinear least squares fitting to multiple exponentials. The quality of these fits were characterized by χ^2 . Additional information is available in [44].

BLI (biolayer interferometry) experiments were conducted essentially as described in [27]. Briefly, biotinylated CaM was immobilized on streptavidin sensors. After establishing a baseline in binding buffer (10 mM HEPES, pH 7.4, 100 mM NaCl, 10% glycerol, 10 μM CaCl₂ and 0.05% surfactant P-20), sensors were moved to binding the buffer containing eNOS for 180 s. Sensors were then moved to the buffer only to monitor dissociation for 180 s. Non-specific binding was measured by immersing sensors without CaM in analyte and was negligible in all cases. All biosensing experiments were performed at 25 °C.

SPR (surface plasmon resonance) experiments were conducted on a Biacore X100 instrument using a biotin CAPture chip. Biotinylated CaM (~150 RU in all cases) was immobilized prior to single-cycle kinetics performed in the binding buffer.

RESULTS

Figure 1 shows the alignment of the DNA and amino acid sequences of mammalian NOS (nitric oxide synthase) isoforms in a region corresponding to an α – β turn within the Rossmann-fold FMN-binding domain. The signal generators eNOS and

conserved AI region		ERK	PKB/Akt	helix			
hnNOS	TGAGGCACCC	C...AACTCT	GTG.....C	AGGAAGAAAG	GAAGAGCTAC	AAGGTCCGAT	2548
rNOS	TGAGGCACCC	C...AACTCT	GTG.....C	AGGAGGAGAG	AAAGAGCTAC	AAGGTCCGAT	2533
heNOS	TGTCCGGCCC	CTACAACAGC	TCCCCTCGGC	CGGAACAGCA	CAAGAGTTAT	AAGATCCGCT	1867
beNOS	TGTCCGGGCC	CTACAACAGC	TCCCCTCGGC	CGGAACAGCA	CAAGAGTTAC	AAGATCCGCT	1873
INOS	TGAAAGAGCT	CAACAAC...	1851
hnNOS	~R~H~P~	~...N~S~	V~.....Q	~E~E~R~	~K~S~Y~	~K~V~R~F~	850
rNOS	~R~H~P~	~...N~S~	V~.....Q	~E~E~R~	~K~S~Y~	~K~V~R~F~	845
heNOS	~S~G~P~	~Y~N~S~	S~P~R~P~	~E~Q~H~	~K~S~Y~	~K~I~R~F~	613
beNOS	~S~G~P~	~Y~N~S~	S~P~R~P~	~E~Q~H~	~K~S~Y~	~K~I~R~F~	615
INOS	~K~E~L~	~N~N~...	617
			frame shift	MAPK binding site			
hnNOS	TCAACAGCGT	CTCCTCCTAC	TCTGACTCCC	AAAAATCATC	.AGGCGATGG	GCCCACCTC	2607
rNOS	TCAACAGCGT	CTCCTCCTAT	TCTGACTCCC	GAAAGTCATC	.GGGCGACGG	ACCCGACCTC	2592
heNOS	TCAACAGCAT	CTCCTGC...	TCAGACCCAC	TGGTGTCCTC	TTGGCGGCGG	AAGAGGAAGG	1925
beNOS	TCAACAGCGT	CTCCTGC...	TCAGACCCGC	TGGTGTCCTC	CTGGCGGCGG	AAGAGAAAGG	1920
INOS
hnNOS	~N~S~V~	~S~S~Y~	S~D~S~Q~	~K~S~S~	~G~D~G~	~P~D~L~	869
rNOS	~N~S~V~	~S~S~Y~	S~D~S~R~	~K~S~S~	~G~D~G~	~P~D~L~	864
heNOS	~N~S~I~	~S~C~..	S~D~P~L~	~V~S~S~	~W~R~R~	~K~R~K~E~	632
beNOS	~N~S~V~	~S~C~..	S~D~P~L~	~V~S~S~	~W~R~R~	~K~R~K~E~	634
INOS
PKA/AMPK		frame resumes					
hnNOS	AGAGA..CAA	CTTTGAGAGT	GCTGGACCCC	TGGCCAATGT	GAGGTTCTCA	GTTTTTGG	2663
rNOS	AGAGA..CAA	CTTTGAAAGT	ACTGGACCCC	TGGCCAATGT	GAGGTTCTCA	GTGTTCCG	2648
heNOS	AGTCCAGTAA	CACAGACAGT	GCAGGGGCC	TGGGCACCT	CAGGTTCTGT	GTGTTCCG	1952
beNOS	AGTCCAGCAA	CACAGACAGT	GCGGGGGCCC	TGGGGACCT	CAGGTTCTGT	GTGTTCCG	1958
INOSAAATT	CAGGTACGCT	GTGTTTGG	1874
hnNOS	R~D~..N~	~F~E~S~	A~G~P~L~	~A~N~V~	~R~F~S~	V~F~G~	888
rNOS	R~D~..N~	~F~E~S~	T~G~P~L~	~A~N~V~	~R~F~S~	V~F~G~	883
heNOS	~S~S~N~	~T~D~S~	A~G~A~L~	~G~T~L~	~R~F~C~	V~F~G~	651
beNOS	~S~S~N~	~T~D~S~	A~G~A~L~	~G~T~L~	~R~F~C~	V~F~G~	653
INOSK~F~	~R~Y~A~	V~F~G~	625

Figure 1 Sequence alignment of NOS mammalian isoforms in the AI element region

Note conserved region (bold) and frame shifts causing divergence of the variable region in eNOS and nNOS. Helix residues are underlined. Phosphorylation sites for ERK, Akt and PKA/AMPK (adenosine monophosphate-activated protein kinase) and the binding site for MAPKs (ERK, p38) are marked with bold italics. Human sequences are denoted by h, rat sequences by r and bovine sequences by b. All DNA sequences numbered from the first base of the start codon in the most commonly studied splice form. Accession numbers for DNA: hnNOS, D16408; rnNOS, X59949; heNOS, M93718; beNOS, M99057; hiNOS, L24553. Protein accession numbers: hnNOS, P29475; rnNOS, P29476; heNOS, P29474; beNOS, P29473; hiNOS, P35228.

nNOS (neuronal nitric oxide synthase) differ from the cytokine induced isoform iNOS (inducible nitric oxide synthase) in that they have an extended insertion at this point that serves as an AI element displaced by CaM binding to a spatially adjacent site [23].

The N-terminal half of the AI, shown in bold, contains a conserved helical region (underlined residues) that locks down the FMN-binding domain through hydrogen bonds to both the FMN-binding domain and the NADPH-binding domain. This prevents conformational changes that are an obligatory part of the catalytic cycle. Ser⁶¹⁷ and Ser⁶³⁵ in bovine eNOS (Ser⁶¹⁵ and Ser⁶³³ in human eNOS) are phosphorylated by kinases [Akt (also known as PKB (protein kinase B)) and PKA] that activate the enzyme; Ser¹¹⁷⁹ in the inhibitory C-terminal extension is a target of the same kinases [15–18].

Recently we reported that MAPKs bind to a pentabasic sequence present in eNOS but not nNOS [38]. This site, shown in bold italics, confers 80 pM affinity for p38 and 160 nM for ERK. The location in this regulatory region suggests interactions between MAPKs and other modulators of eNOS activity.

The evolutionary origin of the MAPK-binding site is implied by the frame shift in the eNOS sequence in comparison to nNOS at the end of the conserved AI region [38]. As shown in Figure 1, a compensating shift restores the reading frame 27 bp later in eNOS, and the homology at the amino acid level immediately resumes. During the 27 bp frame shift, there is however no relationship between eNOS and nNOS at the amino acid level (some homology appears to persist at the DNA level). Divergence of eNOS from nNOS occurred during or before the development of amphibians, and translation of the nNOS sequence in Figure 1

Sequence	Trypticity	Position	Shared
R.APAPAT#PHAPDHSPAPNS#PTLTPPEGPK.F	Fully	41-69	NO
R.APAPAT#PHAPDHSPAPNSPTLTPPEGPK.F	Fully	41-69	NO
R.APAPATPHAPDHSPAPNS#PTLTPPEGPK.F	Fully	41-69	NO
R.APAPATPHAPDHSPAPNS#PTLTPPEGPKFPR.V	Fully	41-72	NO
R.APAPATPHAPDHSPAPNSPTLTPPEGPK.F	Fully	41-69	NO
F.AAALM*EM*SGPYNSS#PRPEQHK.S	Partially	589-609	NO
A.ALM*EM*SGPYNSS#PRPEQHK.S	Partially	591-609	NO
A.ALMEM*SGPYNSS#PRPEQHK.S	Partially	591-609	NO
L.M*EM*SGPYNSS#PRPEQHK.S	Partially	592-609	NO
A.TPHAPDHSPAPNS#PTLTPPEGPK.F	Partially	46-69	NO

Figure 2 MS results for trypsin digest of ERK phosphorylated eNOS showing phosphorylated peptides

Potential phosphorylation sites are indicated by # symbol. Because ERK phosphorylates TP and SP motifs, the results are uniquely consistent with Ser⁶⁰², Thr⁴⁶ and Ser⁵⁸ phosphorylation, which can account for all the species observed. Asterisks indicate oxidized methionines. No peptides were shared with the unphosphorylated control.

with the appropriate frame shift introduces a basic motif. It seems plausible that these motifs arose by chance and were stabilized during evolution by protein–protein interactions.

Phosphorylation of eNOS by ERK was detected *in vitro* by measurement of ADP; the results showed that during a 1 h incubation, two or three ADP were formed per eNOS monomer, suggesting that multiple sites were phosphorylated. Figure 2 shows the results of MS of tryptic digests of unphosphorylated eNOS and eNOS phosphorylated for 15 min by ERK. Coverage was essentially complete; 35 phosphorylated tryptic peptides were obtained in addition to 3545 unphosphorylated peptides.

Ser⁶⁰² and Thr⁴⁶ were identified unambiguously as phosphorylation sites from the MS results alone, considering that only serine and threonine are potential targets. In addition, the data showed that either Ser⁵⁸ or Thr⁶² was phosphorylated; because MAPKs phosphorylate at SP or TP sites, the third position was unambiguously identified as Ser⁵⁸. No indication of phosphorylation at other sites was observed.

Figure 3(A) shows the structure of the reductase portion of nNOS, corresponding roughly to the C-terminal half of the enzyme [45]. No corresponding eNOS crystal structure is available, but the two enzymes are highly homologous in this region and the conserved structures shown should be nearly identical. The ribbon diagram traces the path of the backbone through the FMN, FAD and NADPH-binding domains, with the cofactors shown in solid render. In this conformation, the FAD and FMN isoalloxazines are in van der Waals contact. At the opposite edge of the FMN-binding domain β sheet, the ends of the AI are exposed at the adjacent ends of an α -helix and a β -strand; the trace appears discontinuous because the chain is too flexible here to have a well-defined structure. The AI helix is visible as a disconnected feature, and is connected to the FMN domain β sheet by a long-disordered loop on the C-terminal side and a short-disordered loop on the N-terminal side. The long loop carries the MAPK-binding site close to the edge of the β -sheet and the adjacent CaM-binding site, accounting for the CaM–MAPK competition, which we previously reported [38]. Ser⁶⁰² is located in the short-disordered loop directly adjacent to the α -helical region that precedes the AI. Ser⁶¹⁷ is located in the AI helix, and Ser⁶³⁵

is in the long-disordered loop between the MAPK-binding site and the β -strand that follows the AI. (These residues correspond to Ser⁶⁰⁰, Ser⁶¹⁵ and Ser⁶³³ in human eNOS.)

Figure 3(B) shows the structure of the eNOS oxygenase domain dimer [46,47]. The haem and BH₄ (tetrahydrobiopterin) cofactors are shown in solid render along with the Zn atom that stabilizes the dimer. Thr⁴⁶ and Ser⁵⁸ are located in a disordered region adjacent to the loops bearing the cysteine residues that coordinate the Zn; the sites of myristoylation and palmitoylation are further towards the N-terminus. This region of the oxygenase domain surface is close to the point where the polypeptide chain leaves the oxygenase domain to form the CaM-binding site, and also reasonably close the site of haem reduction on the opposite monomer.

The results of experiments showing the effect of ERK-mediated phosphorylation on eNOS activity in NO synthesis and cytochrome *c* reduction are summarized in Table 1. These figures suggest inhibition of around 60 %, but the results are slightly complicated by two factors. To obtain a high degree of phosphorylation, it is necessary to incubate eNOS with kinases at 22 °C; during the incubation, control eNOS activity decreases slightly. If phosphorylated eNOS is less stable than unphosphorylated eNOS, we could overestimate inhibition slightly. A more serious problem is the incomplete phosphorylation of eNOS. Although we have several measures of the degree of phosphorylation (e.g., the results of fluorescence decay experiments), we cannot exclude the possibility that a minority population of unphosphorylated eNOS accounts for much of the residual activity.

We are confident that NO synthesis measured spectrophotometrically through the reaction of NO with oxyhaemoglobin is inhibited by at least 50 %. Inhibition was confirmed in end point assays with the Griess reagent. Reduction of ferri-cytochrome *c* by eNOS was monitored at 418 and 550 nm to assess the effect of phosphorylation on electron transfer within the reductase unit. Phosphorylation also inhibits cytochrome *c* reduction by at least 50 %. In both cases, it is possible that phosphorylation reduces the activity by more than 70 %.

Figures 4(A) and 4(B) show the time course of eNOS phosphorylation using Western blotting with a phospho-specific

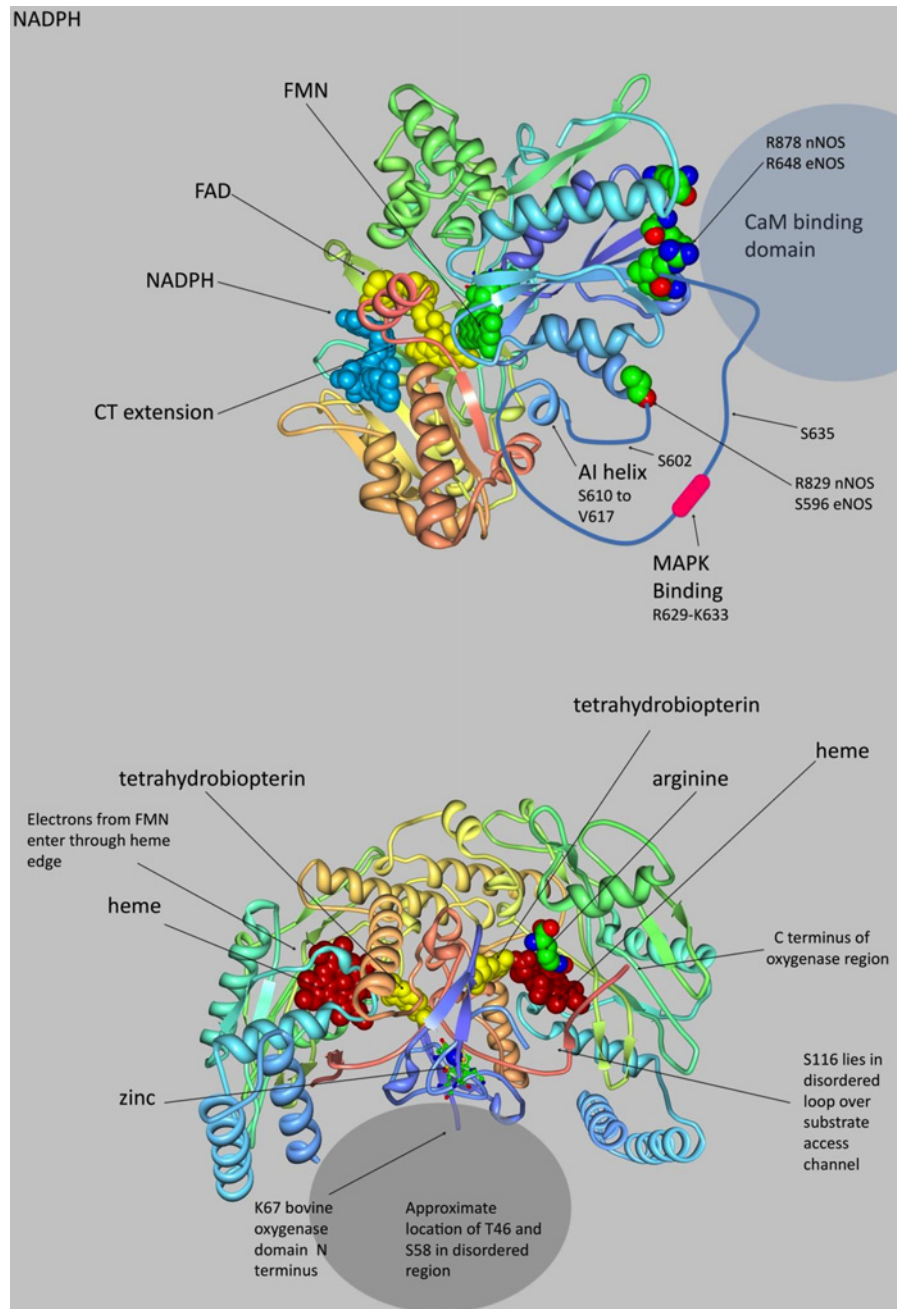


Figure 3 Location of phosphorylation sites in eNOS

(A) Structural cartoon of NOS reductase domains based on the nNOS reductase crystal structure [45]. The FMN-binding domain is in blue, the FAD-binding domain green and the NADPH-binding domain is tan. Cofactors are shown in solid render, and the residues at the N-terminal edge of the FMN-binding domain and at the ends of the AI insertion ($\text{Arg}^{878}/\text{Arg}^{648}$ and $\text{Arg}^{829}/\text{Ser}^{596}$ for nNOS/eNOS) are marked by solid render. The approximate extent and position of the disordered regions of the AI are indicated by a drawn coil. The AI carried previously identified targets for Akt and PKA phosphorylation as well as a MAPK-binding site and a target for ERK phosphorylation (Ser^{602}) that also matches the target motifs of other MAPKs. The C-terminal extension carries Ser^{1179} , a target for Akt and PKA (see PDB 1TLL). (B) Structural cartoon of eNOS oxygenase dimer based on crystal structures [46,47]. The direction of the backbone is indicated by colour, with the N-terminal blue and the ribbon shading through green to tan at the C-terminal. Cofactors and substrate arginine are shown in solid render, with haem shown in red and BH_4 in yellow. The location of two ERK targets in a disordered region at the bottom of the figure is indicated; the region is near the dimer interface. The C-terminal end of the domain is shown emerging from the face at right; this becomes the CaM-binding site, and after a short connector joins the FMN-binding domain shown in Figure 3(A). This domain must supply electrons to the haem at right by disengaging from the reductase complex and re-orienting (see PDB 4NSE and 3NOS).

Table 1 Effects of ERK catalysed phosphorylation of eNOS on activity and on the population of eNOS conformational states characterized by FMN fluorescence lifetimes

The lifetime distributions in this table differ somewhat from those in the fits shown in Figure 5 because they are derived from decays of the CaM-activated enzyme to correspond to NO synthase activity. The distributions in Figure 5 show the effects of phosphorylation in the absence of CaM.

	NO synthesis (nm ⁻¹ min ⁻¹ mg ⁻¹)	Cytochrome c reduction (min ⁻¹)	Fluorescence lifetime (% state populations)		
			90 ps	0.9 ns	4.3 ns
eNOS	110 (10)	143 (20)	53.45	20.21	26.35
eNOS + ERK	42 (7.6)	55 (5)	85	–	15

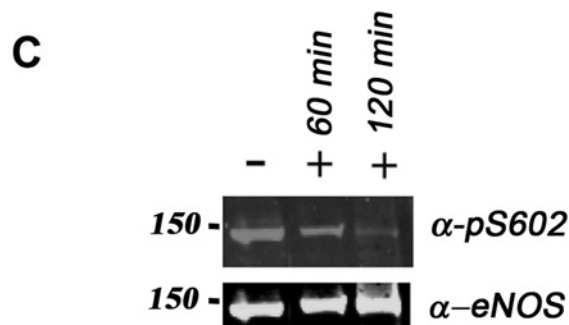
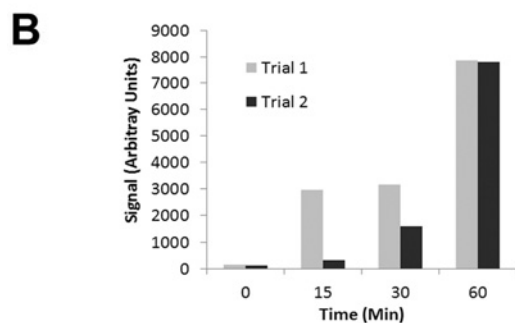
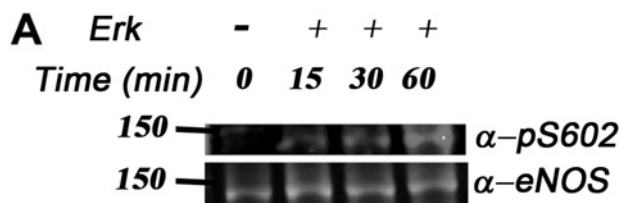


Figure 4 Time course of Ser⁶⁰² phosphorylation and dephosphorylation

(A) Western blots of purified eNOS after 0, 15, 30 and 60 min treatment with ERK showing the development of a band corresponding to phosphorylated Ser⁶⁰² when probed with phospho-specific Ser⁶⁰². Control probed with anti-eNOS shows that lanes are equally loaded and that eNOS is not significantly lost at times up to 1 h, but at longer times the signal from anti-eNOS is markedly reduced. (B) Plot of densitometry from two trials of time course. (C) Western blots of BAEC lysates treated with λ phosphatase and probed with anti-pS602 and anti-eNOS.

pS602 antibody raised to a phosphorylated target peptide and depleted of unspecific components by treatment with unphosphorylated peptide. After a lag of approximately 10 min, ERK phosphorylates eNOS with maximum intensity obtained at about

Table 2 Rate and equilibrium constants for CaM binding to unphosphorylated and ERK phosphorylated eNOS

	– ERK	+ ERK
<i>BLI (single-state)</i>		
k_{on} (M ⁻¹ s ⁻¹)	1.2×10^5	1.2×10^5
k_{off} (s ⁻¹)	1.1×10^{-4}	3.3×10^{-4}
K_D (pM)	920	2700
<i>SPR (sequential model)</i>		
k_{on1} (M ⁻¹ s ⁻¹)	6.4×10^4	1.1×10^5
k_{off1} (s ⁻¹)	2.0×10^{-3}	2.5×10^{-3}
k_{on2} (s ⁻¹)	8.4×10^{-3}	3.7×10^{-3}
k_{off2} (s ⁻¹)	1.9×10^{-4}	1.1×10^{-4}
K_D (pM)	720	650

1 h. By 90 min, the control blot with anti-eNOS was significantly lower, and this was reflected in a weaker signal with anti-pS602.

Figure 4(C) shows Western blots of BAEC lysates probed with anti-pS602 and anti-eNOS after treatment with λ phosphatase. A strong band from eNOS phosphorylated at Ser⁶⁰² is removed by the phosphatase over a period of 2 h, during which the anti-eNOS signal is essentially invariant. This demonstrates that Ser⁶⁰² is significantly phosphorylated in endothelial cells, and that the anti-pS602 antibody does not bind to unphosphorylated eNOS.

We previously showed that CaM binding to unphosphorylated eNOS was diffusion limited and that PKC inhibition of eNOS via phosphorylation at Thr⁴⁹⁷ strongly inhibits CaM binding [27]. ERK phosphorylation of the target residues does not strongly affect CaM binding, suggesting that PKC and ERK inhibit eNOS via different mechanisms. Optical biosensing experiments demonstrate near-1 nM affinities regardless of phosphorylation state. Figures 5(A) and 5(B) show BLI traces with fits to global single-state models for CaM binding to unphosphorylated and phosphorylated eNOS, respectively. Rate constants are shown in Table 2. At the concentrations examined binding can be well approximated by a single-state first-order model with remarkably similar profiles regardless of phosphorylation. The difference in affinity observed is entirely due to a 3-fold higher k_{off} , though this may not be physiologically relevant (see the Discussion section).

Single-cycle kinetic analysis by SPR also revealed that CaM binding of unphosphorylated eNOS in Figure 5(C) is highly similar to phosphorylated (Figure 4D). CaM was immobilized prior to injection of the analyte eNOS. Fits to a sequential model

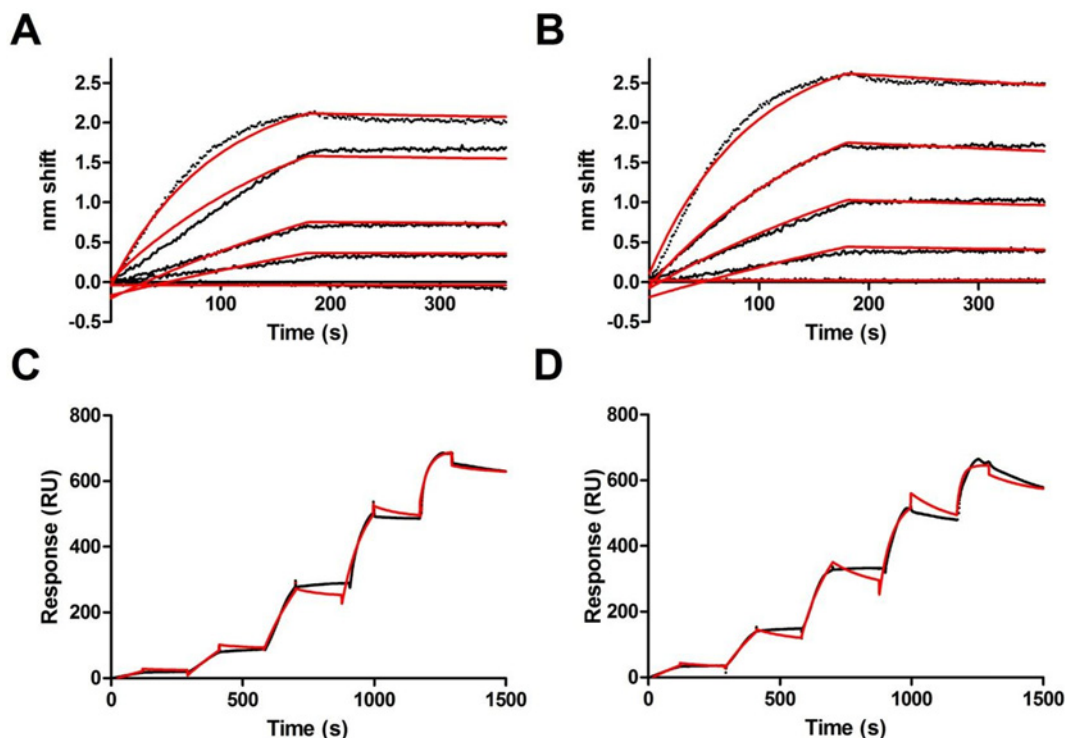


Figure 5 Optical biosensing analysis of CaM-eNOS binding

(A) BLI sensorgram of CaM binding to 0, 10.9, 31.9, 43.7 and 87.5 nM unphosphorylated eNOS. Raw data are in black; fits to a single-state association-then-dissociation model are shown in grey. (B) Same as in (A), but for the same concentrations of phosphorylated eNOS. (C) SPR sensorgram of single-cycle kinetics of tethered CaM binding to 6.2, 18.5, 55.6, 167 and 500 nM analyte unphosphorylated eNOS. Reference-subtracted raw data are in shown in black along with fits to a two-state sequential model in red. (D) Same as in (C), but with phosphorylated eNOS.

(A + B ↔ AB ↔ AB*) generate K_D s similar to those determined from BLI (Table 2), indicating that the secondary event is a minor component.

We recently showed that iNOS passes through a series of obligatory conformational states during its catalytic cycle, including an input state in which the FMN-binding domain is closely associated with the FAD and NADPH-binding domains, an output state in which the FMN-binding domain is associated with the haem-containing oxygenase domain, and a series of open conformations in which FMN is not closely coupled to other prosthetic groups [43]. These states can be resolved by their very different fluorescence lifetimes; eNOS and nNOS have similar conformational states. CaM activation of eNOS and nNOS results in increased levels of the output and open states relative to the closed input state.

Figure 6 shows fluorescence decays of unphosphorylated and ERK-phosphorylated eNOS in the presence and absence of CaM. ERK phosphorylation causes an increase in the input state, which has a lifetime of 90 ps because of close coupling between FMN and FAD, and a concomitant increase in the output state (0.9 ns lifetime) and the open states (4.3 ns average lifetime). This effect is in opposition to the effect of CaM binding, and accounts for the inhibition of NO synthesis and cytochrome *c* reduction by ERK-mediated phosphorylation.

The effects of ERK phosphorylation on eNOS activity and on the distribution of conformational states characterized by FMN fluorescence lifetimes are summarized in Table 1. The effects of ERK phosphorylation on the conformational manifold are opposite of the principal activator, CaM. Apparent inhibition of both NO synthesis and cytochrome *c* reduction is at least 60%, and may be greater because we are unable to phosphorylate eNOS completely without long incubations that damage the enzyme. Fluorescence data and information gained from phospho-specific antibody work suggest that the enzyme is at least 75% phosphorylated.

DISCUSSION

The MAPKs, ERK and p38 are believed to participate in negative feedback signalling networks with eNOS, and good evidence indicates direct phosphorylation of eNOS by ERK in BAECs [35]. Based on indirect evidence obtained in intact cells, sites have been proposed for ERK phosphorylation including Ser¹¹⁶, Thr⁴⁹⁷ and Ser⁶³⁵ [36,37]. Of these, only Ser¹¹⁶ has the SP/TP motif associated with MAPK targets. Ser¹¹⁶ is located on the oxygenase

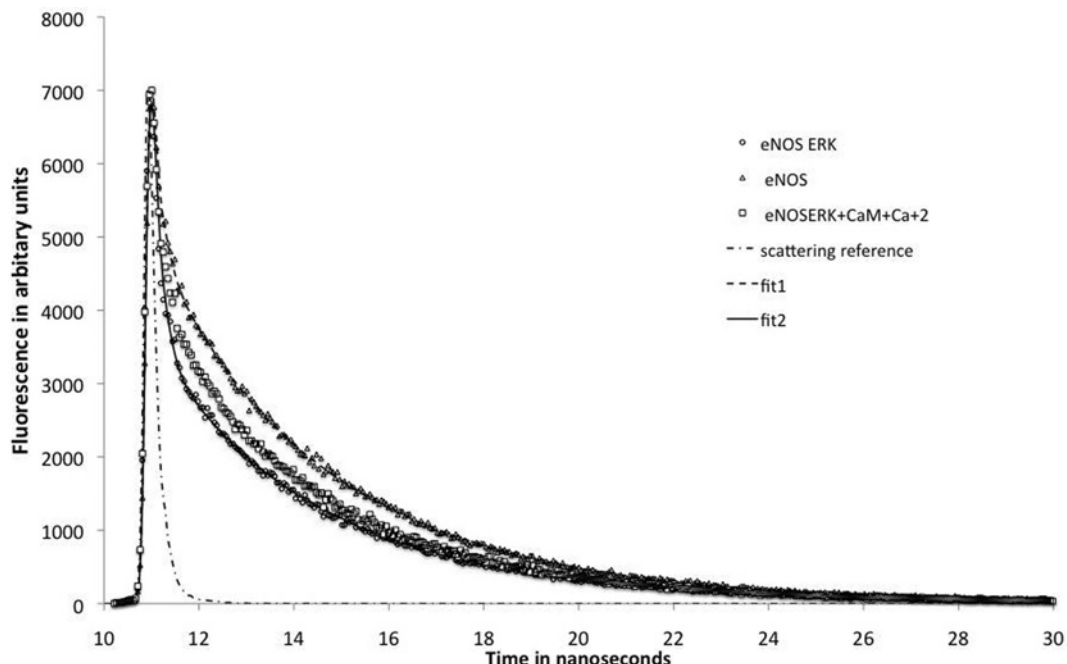


Figure 6 Fluorescence decays of eNOS holoenzyme FMN excited at 473 nm and detected at 525 nm. The eNOS concentrations in the samples were 1 μ M, and were from the same preparation. ERK phosphorylation favours conformational states with shorter lifetimes; CaM activation produces the opposite effect and as shown here partially reverses the effect of ERK phosphorylation. Fitting parameters were: unphosphorylated eNOS: 90 ps, 78%; 3.65 ns, 20%; 0.9 ns, 0.68%; 10.1 ns, 1.6%; $c^2 = 1.10$. ERK phosphorylated eNOS: 80 ps, 86%; 3.83 ns, 12.4%; 1.1 ns 1.8%. All experiments were performed six times using at least two different preparations. The scattering reference was collected at 475 nm, and indicates the width of the exciting pulse.

domain, and the MAPK-binding site we recently identified [27] is located on the AI element of the FMN-binding domain. Phosphorylation of other residues (Thr⁴⁹⁷, Ser⁶³⁵ and human cognates) is the result of pathway dependent ERK-linked activation of other serine–threonine kinases.

Direct *in vitro* phosphorylation of purified eNOS with purified ERK confirmed that eNOS is a substrate for ERK, and further showed that phosphorylation did not require additional scaffolds or adaptors [35]. ERK phosphorylation inhibits both NO synthesis and cytochrome *c* reduction, indicating that phosphorylation interferes with electron transfer reactions mediated by FMN.

Three sites of phosphorylation on eNOS were identified; Ser⁶⁰², at the N-terminal end of the AI, is spatially adjacent to the MAPK-binding site and the CaM-binding site, and is well positioned to interact with other control sites. A ‘lockdown’ of the FMN-binding domain is suggested by fluorescence results showing that phosphorylation pulls the enzyme’s conformational distribution towards the input state. This accounts for the observed inhibition, and suggests that the negatively charged phosphate group stabilizes the input conformation. CaM appears to bind strongly to ERK phosphorylated eNOS, but is unable to effectively override phosphorylation imposed inhibition. Although the results of CaM activation and ERK phosphorylation on the

fluorescence profile are fortuitously opposite ([49] and present communication), we point out that effects on the conformational equilibria are secondary to the changes in rates for conformational transitions. It is possible to inhibit the enzyme by locking it into any conformation, because the mechanism depends on conformational cycling [48].

Our previous report described in detail the complex kinetics of CaM–eNOS binding [27]. In the present study, ERK-phosphorylated eNOS demonstrated a similar CaM-binding profile; diffusion-limited association, very slow dissociation and picomolar affinity. A 3-fold slower dissociation rate constant in BLI accounts for the affinity difference between unphosphorylated and phosphorylated eNOS. The difference may be kinetically significant (95% confidence intervals for k_{off} do not overlap) but cannot account for differences in regulation of NOS activities. The difference in k_{off} is much less pronounced in SPR experiments and the affinities are nearly identical to the 650 pM previously reported [27]. In contrast, phosphorylation of Thr⁴⁹⁷ by PKC interferes with CaM binding [27]. The modes of ERK and PKC inhibition are thus entirely different: PKC prevents the binding of an activator, while ERK interrupts the catalytic cycle.

ERK phosphorylates eNOS at Thr⁴⁶, Ser⁵⁸ and Ser⁶⁰²; the first two of these residues are located in the N-terminal extension of the oxygenase domain. The location of Ser⁶⁰² is ideal for the

control of FMN-mediated electron transfer, and it lies close to the D-domain-type MAPK-binding site. The significance of Thr⁴⁶ and Ser⁵⁸ phosphorylation is unclear. The disordered N-terminal region is known to participate in protein–protein interactions, protein trafficking and myristoylation/palmitoylation. It is unclear that ERK bound to the AI pentabasic site can phosphorylate sites on the oxygenase domain.

We think it unlikely that MAPKs phosphorylate residues such as Thr⁴⁹⁷, Ser⁶¹⁷, Ser⁶³⁵ and Ser¹¹⁷⁹. All these sites with the exception of Thr⁴⁹⁷ activate eNOS, and none of them has an SP or TP target motif [50,51]. When phosphorylation of these sites correlates with MAPK activation, it is likely that this occurs in a pathway-dependent manner. For inhibitory events such as Thr⁴⁹⁷ phosphorylation, this might represent parallel pathways of inhibition. For activating events, it probably represents feedback pathways involved in push–pull regulation.

We were surprised not to detect Ser¹¹⁶ phosphorylation. This residue is located on a flexible loop near the mouth of the substrate access channel of the oxygenase domain, is phosphorylated by SP-directed kinases *in vivo* and has been linked to ERK in plausible studies [37]. Several possibilities present themselves: phosphorylation could be mediated by other kinases, phosphorylation by MAPKs could require additional input (e.g., prior phosphorylation of other sites), or phosphorylation by MAPKs could require scaffolding components.

The tight spacing of control sites on the eNOS surface paints a picture of a system in which eNOS is at the junction of many signalling pathways and is an active node in the resulting network. A simple example of multiple inputs is Thr⁴⁹⁷ phosphorylation, which interferes with CaM binding and hence activation [24,27]. The sites associated with the AI are far more complex. Activating kinases such as PKA and Akt phosphorylate multiple targets in this region (12–18), which also includes the ERK/p38-binding site, the Ser⁶⁰² ERK target and the AI helix, which locks the FMN-binding domain to the NADPH-binding domain. It is likely that phosphorylation of these sites affects the binding of other regulators and phosphorylation of other sites. The complexity of the system may allow eNOS to behave more like an integrated circuit with multiple inputs and a nuanced array of outputs than a simple relay.

AUTHOR CONTRIBUTION

John Salerno wrote the initial draft, provided figures, designed experiments and carried out fluorescence experiments. Dipak Ghosh and Raj Razdan carried out protein biochemistry and assays with eNOS. Katy A. Helms and Emily A. Rye performed kinase experiments and Western blots. Christopher C. Brown performed biosensing experiments on a Forte interferometer. Jonathan L. McMurry participated in experimental design, provided text and figures, did final editing of manuscript and worked on biosensing. Carol A. Chrestensen designed experiments, and carried out kinase experiments, Western blots and endothelial cell experiments. She provided text and figures, and was involved in the final editing of the manuscript.

FUNDING

This work was supported by the National Science Foundation [grant numbers NSF 0950920 (to J.C.S.), NSF CHE0922699 (to J.L.M.) and NSF 1020261 (to C.A.C)] and the National Institutes of Health [grant number NIH R15 GM080701 (to J.L.M.)].

REFERENCES

- Cirit, M., Wang, C.-C. and Haugh, J. M. (2010) Systematic quantification of negative feedback mechanisms in the extracellular signal-regulated kinase (ERK) signaling network. *J. Biol. Chem.* **285**, 36736–36744 [CrossRef PubMed](#)
- Geetha, N., Mihaly, J., Stockenhuber, A., Blasi, F., Uhrin, P., Binder, B. R., Freissmuth, M. and Breuss, J. M. (2011) Signal integration and coincidence detection in the mitogen-activated protein kinase/extracellular signal-regulated kinase (ERK) cascade: concomitant activation of receptor tyrosine kinases and of Lrp-1 leads to sustained ERK phosphorylation via down-regulation of dual specificity phosphatases (Dusp1 and -6). *J. Biol. Chem.* **288**, 25663–25974 [CrossRef](#)
- Krüger, M., Kratchmarova, I., Blagoev, B., Tseng, Y. H., Kahn, C. R. and Mann, M. (2008) Dissection of the insulin signaling pathway via quantitative phosphoproteomics. *Proc. Natl. Acad. Sci. U.S.A.* **105**, 2451–2456 [CrossRef PubMed](#)
- Berridge, M. J., Lipp, P. and Bootman, M. D. (2000) The versatility and universality of calcium signalling. *Nat. Rev. Mol. Cell. Biol.* **1**, 11–21 [CrossRef PubMed](#)
- Furchgott, R. F. (1988) Vascular smooth muscle, peptides, autonomic nerves and endothelium. In *Vasodilation* (Vanhouette, P. M., ed.), pp. 401–404, Raven Press, New York
- Ignarro, L. J., Buga, G. M., Wood, K. S., Byrns, R. E. and Chadhuri, G. (1987) Endothelium derived relaxing factor produced and released from artery and vein is nitric oxide. *Proc. Natl. Acad. Sci. U.S.A.* **24**, 9265–9269 [CrossRef](#)
- Papapetropoulos, A., García-Cardeña, G., Madri, J. A. and Sessa, W. C. (1997) Nitric oxide production contributes to the angiogenic properties of vascular endothelial growth factor in human endothelial cells. *J. Clin. Invest.* **100**, 3131–3139 [CrossRef PubMed](#)
- Ziche, M., Morbidelli, L., Masini, E., Amerini, S., Granger, H. J., Maggi, C. A., Geppetti, P. and Ledda, F. (1994) Nitric oxide mediates angiogenesis *in vivo* and endothelial cell growth and migration *in vitro* promoted by substance P. *J. Clin. Invest.* **94**, 2036–2044 [CrossRef PubMed](#)
- Gaston, B., Drzen, J. M., Loscalzo, J. and Stamler, J. S. (1994) The biology of nitrogen oxides in the airways. *Am. J. Respir. Crit. Care Med.* **149**, 538–551 [PubMed](#)
- Rastaldo, R., Pagliaro, P., Cappello, S., Penna, C., Mancardi, D., Westerhof, N. and Losano, G. (2007) Nitric oxide and cardiac function. *Life Sci.* **81**, 779–793 [CrossRef PubMed](#)
- Abu-Soud, H. M. and Stuehr, D. J. (1993) Electron transfer in the nitric-oxide synthases. Nitric oxide synthases reveal a role for calmodulin in controlling electron transfer. *Proc. Natl. Acad. Sci. U.S.A.* **90**, 10769–10772 [CrossRef PubMed](#)
- Dudzinski, D. and Michel, T. (2007) Life history of eNOS: partners and pathways. *Cardio. Res.* **75**, 247–260 [CrossRef](#)
- Boo, Y. C., Kim, H. J., Song, H., Fulton, D., Sessa, W. and Jo, H. (2006) Coordinated regulation of endothelial nitric oxide synthase activity by phosphorylation and subcellular localization. *Free Rad. Biol. Med.* **41**, 144–153 [CrossRef](#)



- 14 Mount, P. F., Kemp, B. E. and Power, D. A. (2007) Regulation of endothelial and myocardial NO synthesis by multi-site eNOS phosphorylation. *J. Mol. Cell. Cardiol.* **42**, 271–279 [CrossRef PubMed](#)
- 15 Fulton, D., Gratton, J. P. and Sessa, W. C. (2001) Post-translational control of endothelial nitric oxide synthase: why isn't calcium/calmodulin enough? *J. Pharmacol. Exp. Ther.* **299**, 818–824 [PubMed](#)
- 16 Fulton, D., Gratton, J. P., McCabe, T. J., Fontana, J., Fujio, Y., Walsh, K., Franke, T. F., Papapetropoulos, A. and Sessa, W. C. (1999) Regulation of endothelium-derived nitric oxide production by the protein kinase, Akt. *Nature* **399**, 597–601 [CrossRef PubMed](#)
- 17 Michell, B. J., Harris, M. B., Chen, Z. P., Ju, H., Venema, V. J., Blackstone, M. A., Huang, W., Venema, R. C. and Kemp, B. E. (2002) Identification of regulatory sites of phosphorylation of the bovine endothelial nitric-oxide synthase at serine 617 and serine 635. *J. Biol. Chem.* **277**, 42344–42351 [CrossRef PubMed](#)
- 18 Tran, Q. K., Leonard, J., Black, D. J. and Persechini, A. (2008) Phosphorylation within an autoinhibitory domain in endothelial nitric oxide synthase reduces the Ca²⁺ concentrations required for calmodulin to bind and activate the enzyme. *Biochemistry* **47**, 7557–7566 [CrossRef PubMed](#)
- 19 Roman, L. J. and Masters, B. S. (2006) Electron transfer by neuronal nitric-oxide synthase is regulated by concerted interaction of calmodulin and two intrinsic regulatory elements. *J. Biol. Chem.* **281**, 23111–23118 [CrossRef PubMed](#)
- 20 Lane, P. and Gross, S. S. (2002) Disabling a C-terminal autoinhibitory control element in endothelial nitric-oxide synthase by phosphorylation provides a molecular explanation for activation of vascular NO synthesis by diverse physiological stimuli. *J. Biol. Chem.* **277**, 19087–19094 [CrossRef PubMed](#)
- 21 Roman, L. J. and Masters, B. S. S. (2006) Electron transfer by neuronal nitric-oxide synthase is regulated by concerted interaction of calmodulin and two intrinsic regulatory elements. *J. Biol. Chem.* **281**, 23111–23118 [CrossRef PubMed](#)
- 22 Roman, L. J., Martásek, P., Miller, R. T., Harris, D. E., de La Garza, M. A., Shea, T. M., Kim, J. J. and Masters, B. S. (2000) The C-termini of constitutive nitric-oxide synthases control electron flow through the flavin and heme domains and affect modulation by calmodulin. *J. Biol. Chem.* **275**, 29225–29232 [CrossRef PubMed](#)
- 23 Salerno, J. C., Harris, D. E., Irizarry, K., Patel, B., Morales, A. J., Smith, S. M., Martasek, P., Roman, L. J., Masters, B. S., Jones, C. L. et al. (1998) An autoinhibitory control element defines calcium-regulated isoforms of nitric oxide synthase. *J. Biol. Chem.* **272**, 29769–29777 [CrossRef](#)
- 24 Lin, M. I., Fulton, D., Babbitt, R., Fleming, I., Busse, R., Pritchard, K. A. Jr. and Sessa, W. C. (2003) Phosphorylation of threonine 497 in endothelial nitric-oxide synthase coordinates the coupling of L-arginine metabolism to efficient nitric oxide production. *J. Biol. Chem.* **278**, 44719–44726 [CrossRef PubMed](#)
- 25 Michell, B. J., Chen, Z., Tiganis, T., Stapleton, D., Katsis, F., Power, D. A., Sim, A. T. and Kemp, B. E. (2001) Coordinated control of endothelial nitric-oxide synthase phosphorylation by protein kinase C and the cAMP-dependent protein kinase. *J. Biol. Chem.* **276**, 17625–17628 [CrossRef PubMed](#)
- 26 Fleming, I., Fisslthaler, B., Dimmeler, S., Kemp, B. E. and Busse, R. (2001) Phosphorylation of Thr495 regulates Ca²⁺/calmodulin-dependent endothelial nitric oxide synthase activity. *Circ. Res.* **88**, E68–E75 [CrossRef PubMed](#)
- 27 McMurry, J. L., Chrestensen, C. A., Scott, I. M., Lee, E. W., Rahn, A. M., Johansen, A. M., Forsberg, B. J., Harris, K. D. and Salerno, J. C. (2011) Rate, affinity and calcium dependence of nitric oxide synthase isoform binding to the primary physiological regulator calmodulin. *FEBS J.* **278**, 4943–4954 [CrossRef PubMed](#)
- 28 Cargnello, M. and Roux, P. P. (2011) Activation and function of the MAPKs and their substrates, the MAPK-activated protein kinases. *Microbiol. Mol. Biol. Rev.* **75**, 50–83 [CrossRef PubMed](#)
- 29 Cuadrado, A. and Nebreda, A. R. (2010) Mechanisms and functions of p38 MAPK signaling. *Biochem. J.* **429**, 403–417 [CrossRef PubMed](#)
- 30 Zarubin, T. and Han, J. (2005) Activation and signaling of the p38 MAP kinase pathway. *Cell Res.* **15**, 11–18 [CrossRef PubMed](#)
- 31 Bardwell, A. J., Frankson, E. and Bardwell, L. (2009) Selectivity of docking sites in MAPK kinases. *J. Biol. Chem.* **284**, 13165–13173 [CrossRef PubMed](#)
- 32 Gaestel, M. (2008) Specificity of signaling from MAPKs to MAPKAPKs: kinases' tango. *Nuevo. Front. Biosci.* **13**, 6050–6059 [CrossRef](#)
- 33 Yang, J., Wu, L. J., Tashiro, S., Onodera, S. and Ikejima, T. (2008) Nitric oxide activated by p38 and NF- κ B facilitates apoptosis and cell cycle arrest under oxidative stress in evodiamine-treated human melanoma A375-S2 cells. *Free Radic. Res.* **42**, 1–11 [CrossRef PubMed](#)
- 34 Ridnour, L. A., Isenberg, J. S., Espey, M. G., Thomas, D. D., Roberts, D. D. and Wink, D. A. (2005) Nitric oxide regulates angiogenesis through a functional switch involving thrombospondin-1. *Proc. Natl. Acad. Sci. U.S.A.* **102**, 13147–13152 [CrossRef PubMed](#)
- 35 Bernier, S. G., Haldar, S. and Michel, T. (2000) Bradykinin-regulated interactions of the mitogen-activated protein kinase pathway with the endothelial nitric-oxide synthase. *J. Biol. Chem.* **275**, 30707–30715 [CrossRef PubMed](#)
- 36 Xiao, Z., Wang, T., Qin, H., Huang, C., Feng, Y. and Xia, Y. (2011) Endoplasmic reticulum Ca²⁺ release modulates endothelial nitric-oxide synthase via extracellular signal-regulated kinase (ERK) 1/2-mediated serine 635 phosphorylation. *J. Biol. Chem.* **286**, 20100–20108 [CrossRef PubMed](#)
- 37 Ruan, L., Torres, C. M., Qian, J., Chen, F., Mintz, J. D., Stepp, D. W., Fulton, D. and Venema, R. C. (2011) Pin1 prolyl isomerase regulates endothelial nitric oxide synthase. *Arterioscler. Thromb. Vasc. Biol.* **31**, 392–398 [CrossRef PubMed](#)
- 38 Chrestensen, C. A., McMurry, J. L. and Salerno, J. C. (2012) Map kinases bind endothelial nitric oxide synthase. *FEBS Open Biol.* **2**, 51–55 [CrossRef](#)
- 39 Martasek, P., Liu, Q., Liu, J., Roman, L. J., Gross, S. S., Sessa, W. C. and Masters, B. S. (1996) Characterization of bovine endothelial nitric oxide synthase expressed in *E. coli*. *Biochem. Biophys. Res. Commun.* **219**, 359–365 [CrossRef PubMed](#)
- 40 Ghosh, D. K., Rashid, M. B., Crane, B., Taskar, V., Mast, M., Misukonis, M. A., Weinberg, J. B. and Eissa, N. T. (2001) Characterization of key residues in the subdomain encoded by exons 8 and 9 of human inducible nitric oxide synthase: a critical role for Asp280 in substrate binding and subunit interactions. *Proc. Natl. Acad. Sci. U.S.A.* **98**, 10392–10397 [CrossRef PubMed](#)
- 41 Gross, S. S. (1996) Microtiter plate assay for determining kinetics of nitric oxide synthesis. *Methods Enzymol.* **268**, 159–168 [CrossRef PubMed](#)
- 42 Newman, E., Spratt, D. E., Mosher, J., Cheyne, B., Montgomery, H. J., Wilson, D. L., Weinberg, J. B., Smith, S. M., Salerno, J. C., Ghosh, D. K. and Guillemette, J. G. (2004) Differential activation of nitric-oxide synthase isozymes by calmodulin-troponin C chimeras. *J. Biol. Chem.* **279**, 33547–33557 [CrossRef PubMed](#)
- 43 Ghosh, D. K., Ray, K., Rogers, A. J., Nahm, N. J. and Salerno, J. C. (2012) FMN fluorescence in iNOS constructs reveals a series of conformational states involved in the reductase catalytic cycle. *FEBS J.* **279**, 1306–1317 [CrossRef PubMed](#)
- 44 Lakowicz, J. R. (2006) Principles of Fluorescence Spectroscopy, (3rd ed.), Springer, New York [CrossRef](#)
- 45 Garcin, E. D., Bruns, C. M., Lloyd, S. J., Hosfield, D. J., Tiso, M., Gachhui, R., Stuehr, D. J., Tainer, J. A. and Getzoff, E. D. (2004) Structural basis for isozyme-specific regulation of electron transfer in nitric-oxide synthase. *J. Biol. Chem.* **279**, 37918–37927 [CrossRef PubMed](#)

- 46 Fischmann, T. O., Hruza, A., Niu, X. D., Fossetta, J. D., Lunn, C. A., Dolphin, E., Prongay, A. J., Reichert, P., Lundell, D. J., Narula, S. K. and Weber, P. C. (1999) Structural characterization of nitric oxide synthase isoforms reveals striking active-site conservation. *Nat. Struct. Biol.* **6**, 233–242 [CrossRef](#) [PubMed](#)
- 47 Raman, C. S., Li, H., Martasek, P., Kral, V., Masters, B. S. and Poulos, T. L. (1998) Crystal structure of constitutive endothelial nitric oxide synthase: a paradigm for pterin function involving a novel metal center. *Cell* **95**, 939–950 [CrossRef](#) [PubMed](#)
- 48 Ghosh, D. K. and Salerno, J. C. (2003) Nitric oxide synthases: domain structure and alignment in enzyme function and control. *Front. Biosc.* **8**, D193–D209 [CrossRef](#)
- 49 Salerno, J. C., Ray, K., Poulos, T., Li, H. and Ghosh, D. K. (2013) Calmodulin activates neuronal nitric oxide synthase by enabling transitions between conformational states. *FEBS Lett.* **587**, 44–47 [CrossRef](#) [PubMed](#)
- 50 Ben-Levy, R., Leighton, I. A., Doza, Y. N., Attwood, P., Morrice, N., Marshall, C. J. and Cohen, P. (1995) Identification of novel phosphorylation sites required for activation of MAPKAP kinase-2. *EMBO J.* **14**, 5920–5930 [PubMed](#)
- 51 White, A., Pargellis, C. A., Studts, J. M., Werneburg, B. G. and Farmer, II, B. T. (2007) Molecular basis of MAPK-activated protein kinase 2:p38 assembly. *Proc. Natl. Acad. Sci. U.S.A.* **104**, 6353–6358 [CrossRef](#) [PubMed](#)

Received 21 January 2014/3 July 2014; accepted 4 July 2014

Published as Immediate Publication 7 July 2014, doi 10.1042/BSR20140015
